Proceedings of the 11th International Conference on Fluid Flow, Heat and Mass Transfer (FFHMT 2024)
Chestnut Conference Centre - University of Toronto, Toronto, Canada – June 16-18, 2024
Paper No. 033
DOI: 10.11159/ffhmt24.033

Designing a Comparative Interferometric Method for Measuring the Thermal Conductivity of Transparent Fluids

S. Sahamifar [1], D. Naylor, T. Yousefi, J. Friedman
Department of Mechanical, Industrial, and Mechatronics Engineering, Toronto Metropolitan University
350 Victoria St., Toronto, Canada, M5B 2K3
[1]ssahamifar@torontomu.ca

Abstract – In this paper, a comparative interferometric method is designed to measure the relative thermal conductivity of transparent fluids compared to deionized water by examining temperature fields in both fluids, separated by a thin conductive barrier. The flow and temperature fields in the experimental model were numerically simulated using Ansys Fluent 2023 R1. To minimize natural convection effects, the model was heated from the top and cooled from the bottom. The impact of natural convection within the cavities was investigated by simulating the model with and without considering the natural convection effects. Moreover, various sources of potential experimental errors, such as heat loss to the ambient and imperfect levelling (±0.5 degrees) were examined. The simulated interference fringes (lines of constant beam-averaged temperature) were reconstructed in the numerical model for each case. Subsequently, the simulated fringes were analysed to obtain the temperature gradient in both fluids and the relative thermal conductivity of the test fluid. It was shown that the impact of natural convection on the results is negligible and can be disregarded. Furthermore, all the mentioned error sources lead to less than a 0.2% error in the measured relative thermal conductivity. A sample infinite fringe interferogram from the experimental model is presented for deionized water as both the test and reference fluids. This new comparative optical method will be ultimately used to measure the relative thermal conductivity of nanofluids in support of a program of optical convective heat transfer research.

***Keywords*:** thermal conductivity, CFD, design, transparent fluids, nanofluids, interferometry

1. Introduction

In recent decades, thermal design researchers have strived to find new methods to boost heat transfer rates in response to growing industrial demands. Among these methods, nanofluids have gained more attention in the last two decades [1]. To effectively explore heat transfer studies, a solid understanding of the thermophysical properties of the working fluid is imperative. This study primarily focuses on evaluating the design of an optical model to measure the thermal conductivity of transparent fluids, particularly emphasizing dilute nanofluids. This property is crucial for laser interferometry-based convective heat transfer measurements.

Various techniques have been employed to measure the thermal conductivity of nanofluids. These methods fall into two primary categories: steady-state techniques, including parallel plates [2] and coaxial cylinders [3], and transient methods, containing the transient hot wire [4], transient plane source [5], temperature oscillation [6], laser flash method [7], and 3ω method [8]. Recently, researchers have introduced new techniques by adapting traditional methods [2-8], which reduce the sample size requirements. Two examples of such methods include the modified transient plane source (MTPS) [9] and an extended 3ω method [10]. As seen in the literature, most researchers have utilized non-optical methods for their experiments. However, only two recent studies [11, 12] have employed optical techniques to measure nanofluid thermal conductivity using laser interferometry with a transient conduction inverse method.

Steady-state techniques [2-3] often demand larger samples and longer testing times. On the other hand, transient methods [4-12] involve more complex calculations. Moreover, several of these techniques [2-10] do not provide temperature field visualization, a feature unique to optical methods, which is crucial for analyzing thermal conductivity and heat transfer measurements.

The primary objective of this research is to evaluate the design of an experimental model to conduct a new optical comparative study on transparent fluid thermal conductivity. This study determines relative thermal conductivity by analyzing the steady-state temperature gradients in a test and reference fluid (water) separated by a thin conductive barrier.

Unlike other steady-state methods [2-3], this approach requires less sample volume and a shorter measurement time. Its optical nature enables complete temperature field visualization and minimizes uncertainties associated with thermocouple calibration. Moreover, its comparative design eliminates the necessity for photographic scale adjustments due to consistent image magnification between the test and reference fluids.

The method compares average temperature fields along the beam direction acquired through Mach- Zehnder Interferometry (MZI) in test and reference fluids. In this paper, the temperature fields are numerically reconstructed using ANSYS Fluent 2023 R1 when the reference and test fluids are water. The relative thermal conductivity of water is then determined by utilizing the acquired temperature fields. This numerical simulation allows the assessment of whether free convection influences the accuracy of interferometry measurements. Additionally, the impact of lateral heat transfer on the energy balance at the dividing plate is assessed. The study also explores the effect of imperfect model levelling due to the digital level accuracy. Finally, the temperature fields of the water inside the cavities were visualized for the experimental model.

2. Numerical analysis

The geometry of the numerical model used in this study is illustrated in Fig. 1.a. Moreover, the middle part of the model without optics on the two sides is displayed in Fig. 1.b in detail. As shown in Fig. 1.a, the model comprises two optical windows with λ/10 surface flatness, 50.80 mm diameter, and 12.70 mm thickness, alongside a middle fluid chamber. The middle fluid chamber (Fig. 1.b) includes Delrin plates on the right and left sides of the cavities to minimize heat loss. Aluminum plates at the top and bottom distribute heat to the fluids, and a 2.00 mm thick aluminum plate partitions the cavity into two compartments. One compartment contains the reference fluid, water, and the other holds the test fluid, nanofluid. The volume of both the test and reference fluid samples is 2.7 ml. The optical windows are positioned on either side of the middle section, as depicted in Fig. 1. a. Both fluid cavities possess identical dimensions, with lengths, widths, and optical lengths (in the beam direction) of 30.00, 9.00, and 10.00 mm, respectively.

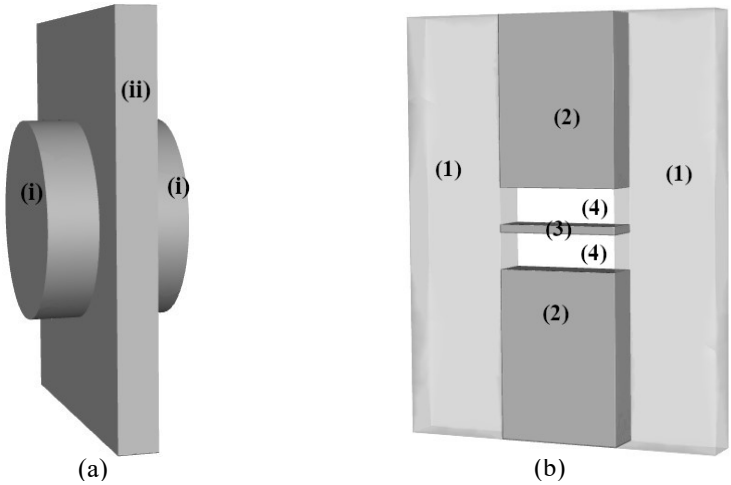

Fig. 1. (a) The geometry of the numerical model: i) the two optics, ii) the middle fluid chamber; (b) the middle fluid chamber: 1) the two Delrin plates, 2) the two aluminum plates, 3) the middle-separating plate, 4) The cavities filled with water or nanofluid

Conduction within the solid components and the heat dissipation from the perimeter of the middle fluid chamber and optics to the surroundings were considered. The thermal conductivities of the solid components are presented in Table 1. The heat is dissipated to the surrounding quiescent air at an average temperature and a convection coefficient of 21.5°C and 10 W / m^2K, respectively. Heat loss in the beam direction (perpendicular to Delrin and Aluminum plates in Fig. 1), excluding the optic parts, has been neglected. In the experimental model, two thick Delrin parts will be positioned on the two sides of the middle fluid chamber to ensure the same conditions as those simulated numerically. Furthermore, the top and bottom Aluminum plates are maintained at a constant temperature of 26.5 and 16.5°C, respectively. All thermophysical properties of water are treated as temperature-dependent properties using Touloukian data [13], except for specific heat capacity (c_p), which remains relatively constant within the temperature range of the domain (16.5-26.5°C).

Table 1. Thermal conductivity of the solid materials used in the study.

Material	Thermal conductivity (W/mK)
Delrin	0.37
Optics	1.38
Aluminum	166

The mesh used in the current numerical simulation is shown in Fig. 2.a. While it is possible to simulate only one-fourth of the model due to its symmetric nature, the entire model was simulated for comparison. This allows for evaluating the scenario with a ±0.5 degrees slope deviation due to levelling imperfections. In this situation, both flow and temperature field may not be entirely symmetric, necessitating the simulation of the entire model.

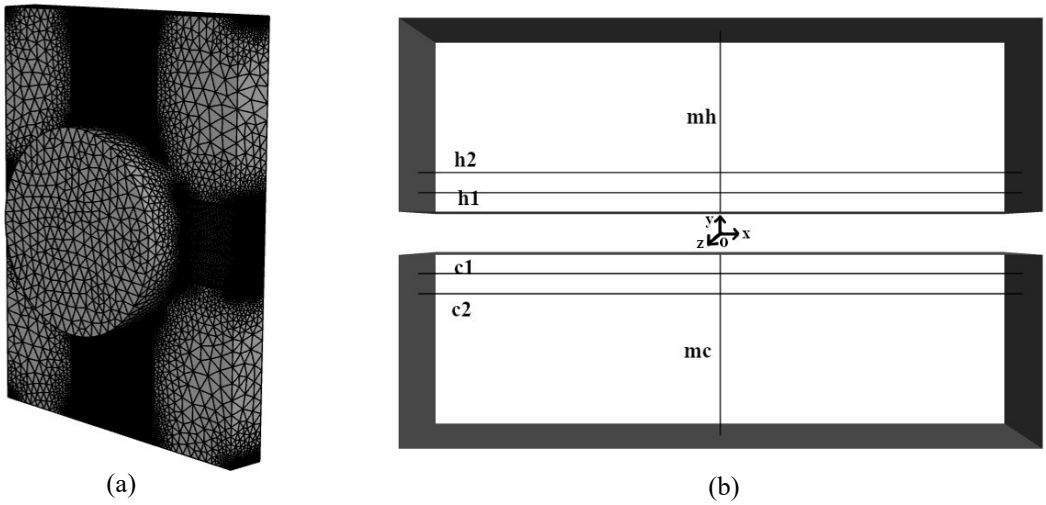

(a) (b)

Fig. 2. (a) The mesh used in the study; (b) the lines defined in the upper and lower cavities (Cavities indicated as (4) in Fig. 1. b)

As shown in Fig. 2.b, the coordinate system is located at the center of the model between the two cavities. Two horizontal lines are defined at different y-coordinates parallel to the middle-separating plate, positioned at the center of the cavities at z=0. In the upper cavity, the distance between the middle-separating plate and the first line is identical to that between the first and second lines. These lines are denoted as h1 and h2. In the lower cavity, two other lines (c1 and c2) are also established, maintaining the same distance from the separating plate as h1 and h2. Optical principles were employed to estimate the approximate number and spacing of fringes to define c1, c2, h1, and h2 lines. The temperature along these lines corresponds to the fringes obtained in the experimental setup, as will be shown in Fig. 7.b. Additionally, two vertical lines, mc and mh, are defined at the center of the cavities at x= z=0 to determine the temperature gradient at different y coordinates within the cavities.

The flow and heat transfer characteristics are attained by solving the continuity, momentum, and energy equations for incompressible flow incorporating the governing boundary conditions. The governing conservation equations are simplified by considering a three-dimensional, steady, incompressible, and laminar convection flow driven by buoyancy. These equations and the boundary conditions are discretized and solved by ANSYS Fluent 2023 R1 software. The convergence criterion is 10^{-9} for all equations. The temperature along the defined lines was also monitored and examined as an additional convergence criterion. A mesh independence analysis was also carried out, demonstrating that the optimal mesh number for the study is 2.29 million. Subsequent increments in the number of meshes did not result in significant changes in the monitored temperatures.

The comparative measurement method is based on the 1D approximation that heat flux from the fluid in the top cavity to the separating plate is equal to that from the separating plate to the fluid in the bottom (reference) cavity at the steady state condition.

$$k_t\left(\frac{dT}{dy}\right)_t = k_{ref}\left(\frac{dT}{dy}\right)_{ref} \quad (1)$$

$$k^* = \frac{k_t}{k_{ref}} = \frac{\left(\frac{dT}{dy}\right)_{ref}}{\left(\frac{dT}{dy}\right)_t} \quad (2)$$

Where k, k^*, and dT/dy represent the thermal conductivity, relative thermal conductivity, and temperature gradient, respectively. The subscripts t and ref stand for test and reference fluids. This paper demonstrates the applicability of the model by employing deionized water as both the test and reference fluids. Water is chosen due to its well-established temperature coefficient of refractive index (dn/dT) [14], which is crucial for optical measurements.

3. Results

Numerical simulations were conducted with and without accounting for natural convection effects. To perform the simulation without accounting for natural convection effects, the gravitational acceleration (g) was set to 0, ensuring that only conduction occurs within the fluid chambers. The temperatures along the lines c1, c2, h1, and h2 are displayed in Fig. 3 for the case where natural convection effects are considered. As shown in Fig. 3, it is evident that the beam-averaged temperatures remain constant on these lines, indicating their alignment with the experimental constant temperature lines (fringes). Additionally, it is observed that temperatures on the two Delrin boundaries exhibit only a minimal deviation compared to other constant temperatures. This slight variation is attributed to the minimal heat loss/gain to/from the ambient in the upper/lower cavities. The temperatures along all defined lines exhibit similar trends and values in the case without considering natural convection effects (pure conduction). For compactness, the corresponding figure is not presented.

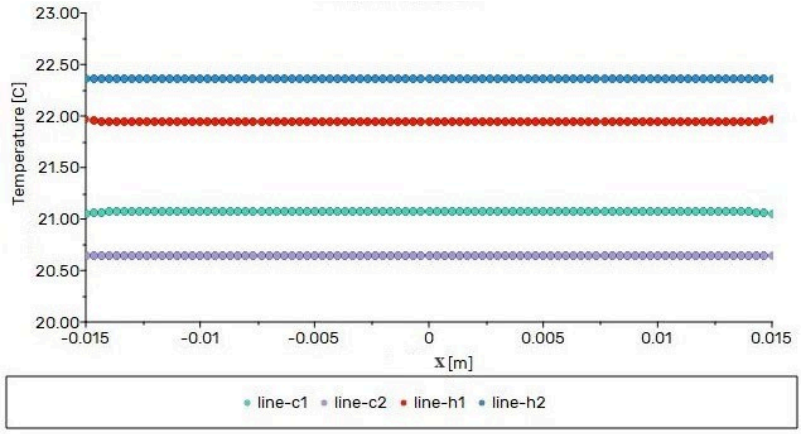

Fig. 3. The z-averaged (beam-averaged) temperatures along c1, c2, h1, and h2 lines defined at different y coordinates parallel to the middle separating plate at z=0.

Temperature differences were calculated for the lines specified in the upper cavity (dT_h) and lower cavity (dT_c) for both scenarios, simulating the model with and without accounting for natural convection effects. Subsequently, these differences were divided by their corresponding distances, 1 mm, to determine the temperature gradient (dT/dy). Using the temperature gradients in conjunction with eq. 2, the relative thermal conductivity of water is determined for both cases, as presented in Table 2. As depicted in Table 2, the difference in relative thermal conductivity between the two scenarios is less than 0.2%, demonstrating a minimal impact of convection and indicating that pure conduction governs the heat transfer within the cavities.

Table 2. Relative thermal conductivities obtained for various cases in the study.

Case	k^*
Without natural convection effects (pure conduction)	0.997
With natural convection effects	0.999
With natural convection effects and considering $\pm 0.5^{\circ}$ leveling imperfection	0.999

Numerical simulations were also conducted by including natural convection effects and introducing a 0.5-degree rotation of the model axis to explore the implications of levelling imperfections. The relative thermal conductivity of water obtained by this configuration is also presented in Table 2. As depicted in Table 2, the discrepancy associated with a 0.5-degree levelling imperfection is almost negligible, confirming that the digital levelling precision adequately suits the study requirements. For water, a perfect measurement should yield a value of k*=1.000. Therefore, given the nearly identical relative thermal conductivity of water from all simulations (close to the ideal value of 1), it demonstrates the model's suitability for measuring the thermal conductivity of water. It should be noted that the relative thermal conductivity being closer to 1 when considering natural convection does not indicate higher accuracy compared to the pure conduction case. The deviation from unity in all cases solely stems from discretization and other pertinent numerical errors.

The temperature variation along the central lines of mc and mh is demonstrated in Fig. 4. The figure illustrates that the temperature changes at a nearly identical slope with respect to y in both upper and lower cavities. This implies that the temperature gradient (dT/dy) remains the same for all horizontal lines specified in the y direction, including c1, c2, h1, and h2. Consequently, apart from these specified lines, any horizontal line designated in the y direction will yield similar results and can be employed for the experimental calculations. Nevertheless, the first two fringes will be utilized in the experimental measurements as they provide a more accurate representation of heat transfer to/from the middle barrier.

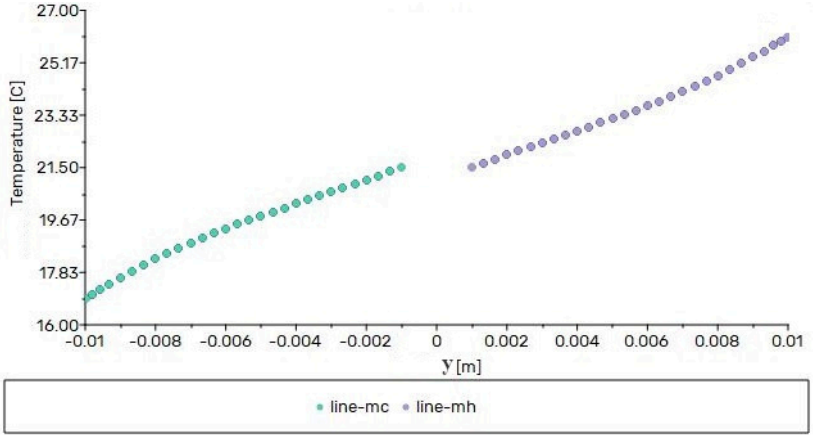

Fig. 4. Beam-averaged temperature variation in the y-direction along the center lines of mc and mh, located at the center of the cavities (x=z=0).

Figure 5 exhibits the velocity vectors and temperature contours for the case in which natural convection effects are considered alongside perfect levelling. It is evident that the prevailing velocity magnitude in the field is in the order of $10^{-5} m/s$, further confirming the negligible influence of natural convection in the model. For brevity, vector, and contour representations for other cases, which closely resemble those presented in Fig. 5, are not shown.

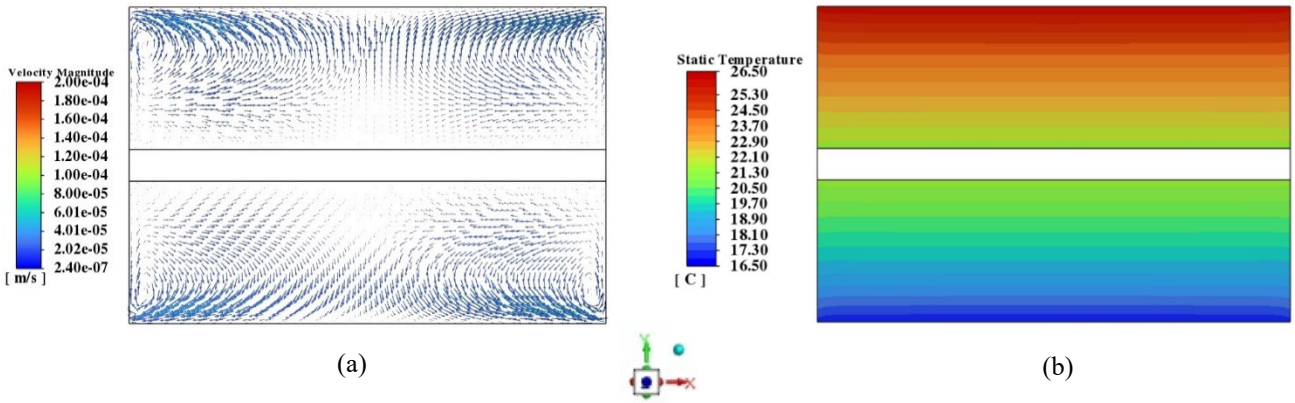

Fig. 5. Vectors and contours at the center of the cavities (z=0) for water-filled upper and lower cavities: (a) velocity vector; (b) contour of temperature

The experimental model constructed for measuring transparent fluid thermal conductivity through the comparative method and a photograph of its components are depicted in Fig. 6. As shown in Fig. 6.b, two thick Delrin end walls are attached to the middle fluid chamber to reduce heat loss to the ambient, as considered in the numerical model. The experimental model was placed in the test beam of a Mach-Zehnder Interferometry (MZI), undergoing heating from the top and cooling from the bottom Aluminum plates. The details of MZI can be found in the literature [15]. The interference fringe pattern before and after applying a 10°C temperature difference is depicted in Fig. 7 a-b for the case where water is injected into both cavities. The infinite interference fringes (horizontal lines) shown in Fig. 7.b correspond to the beam-averaged temperatures along the horizontal lines defined in the numerical model (lines h1, h2, c1, and c2), as depicted in Fig. 3. Details about the experimental model can be found in the recently published journal article [16].

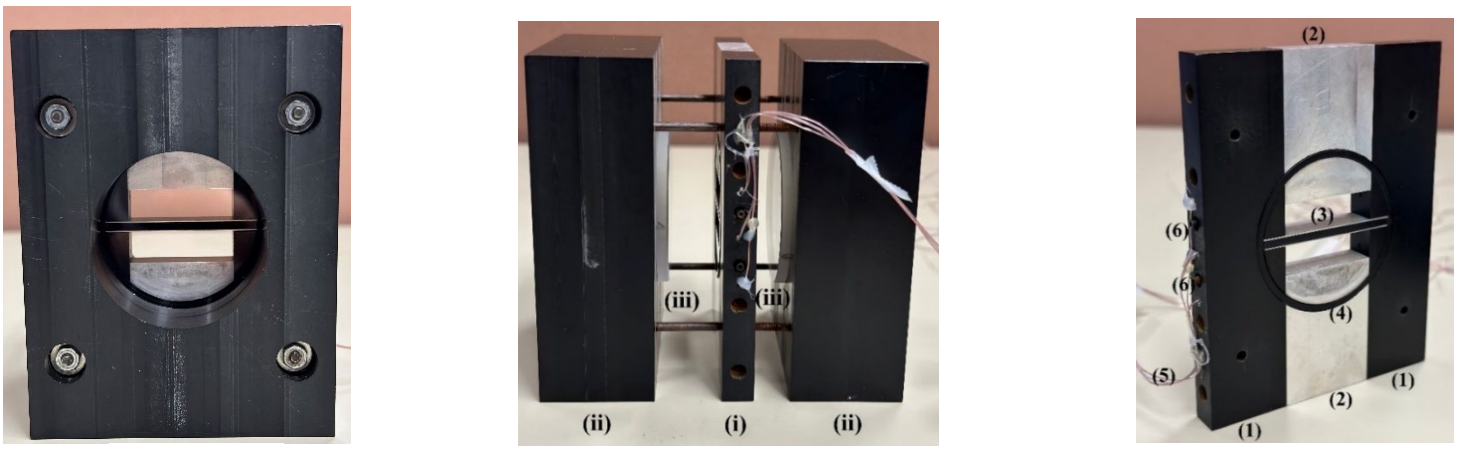

Fig. 6. (a) The front view of the assembled model (b) Parts of the model: i) the middle fluid chamber section, ii) the two Delrin end walls, iii) the two optical windows. (c) Parts of the middle section: 1) the two Delrin plates, 2) the two aluminum plates, 3) the middle-separating plate, 4) O-rings, 5) the thermocouples inserted in their designated holes, 6) the fluid injection holes.

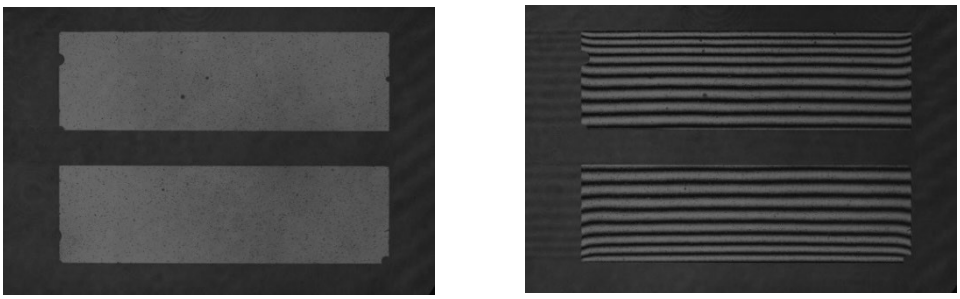

(a) (b)

Fig. 7. Infinite interference fringe patterns for deionized water inside both cavities: (a) initial point (no temperature gradient); (b) after applying temperature difference (steady-state condition)

4. Conclusion

A CFD study has been conducted to assess the accuracy of a new comparative interferometric method to measure the relative thermal conductivity of transparent fluids. The study examined natural convection effects within the cavities filled with deionized water and investigated potential experimental errors, including heat loss to the ambient and a 0.5-degree deflection due to the digital level accuracy of ± 0.5 degrees. It was shown that pure conduction governs the heat transfer inside the cavities, and all the mentioned sources of error contribute to a relative thermal conductivity error of less than 0.2%. An infinite fringe interferogram has been obtained with the experimental model, for water as both the test and reference fluid. This interferogram shows a conduction-dominated temperature field inside the two fluid cavities. This new comparative optical method has been used to measure the relative conductivity of dilute alumina-water nanofluids, as outlined in the recently published journal article. [16].

Acknowledgments

The support of the Natural Sciences and Engineering Research Council of Canada is gratefully acknowledged.

References

[1] M. Sharifpur, "Common Mistakes in Convective Nanofluids Research," in *Proceedings of the 17th International Heat Transfer Conference (IHTC-17)*, 2023, KN 25, pp. 386-404.

[2] M.M. Kostic, C.J. Walleck, "Design of a steady-state, parallel-plate thermal conductivity apparatus for nanofluids and comparative measurements with transient HWTC apparatus," in *ASME 2010 International Mechanical Engineering Congress and Exposition*, 2010, pp. 1457–1464.

[3] B. Barbés, R. Páramo, E. Blanco, C. Casanova, "Thermal conductivity and specific heat capacity measurements of CuO nanofluids," *J. Therm. Anal. Calorim*, 2014, 115, 1883–1891.

[4] A.V. Minakov, V.Y. Rudyak, D.V. Guzei, M.I. Pryazhnikov, A.S. Lobasov, "Measurement of the thermal-conductivity coefficient of nanofluids by the hot-wire method," *J. Eng. Phys. Thermophys*., 88 (1) (2015) 149–162.

[5] Zhu D., Li X., Wang N., Wang X., Gao J., Li H., "Dispersion behavior and thermal conductivity characteristics of Al_2O_3-H2O nanofluids Curr." *Appl. Phys.*, 9 (2009), pp. 131-139.

[6] Das, S.K., Putra, N., Thiesen, P., Roetzel, W., "Temperature Dependence of Thermal Conductivity Enhancement for Nanofluids.," *J. Heat Transf.*, 2003, 125, 567–574.

[7] Zeng, Y.-X., Zhong, X.-W., Liu, Z.-Q., Chen, S., Li, N., "Preparation and Enhancement of Thermal Conductivity of Heat Transfer Oil-Based MoS2 Nanofluids," *J. Nanomater*, 2013, 2013, 270490.

[8] Karthik, R., Harish Nagarajan, R.; Raja, B., Damodharan, P., "Thermal conductivity of CuO-DI water nanofluids using 3-ω measurement technique in a suspended micro-wire," *Exp. Therm. Fluid Sci*, 2012, 40, 1–9.

[9] Vakilinejad A, Aroon MA, Al-Abri M, Bahmanyar H, Myint MTZ, Vakili-Nezhaad GR, "Experimental and theoretical investigation of thermal conductivity of some water-based nanofuids," *Chem Eng Commun*., 2018;205:610–23.

[10] Oh, D.-W, "Thermal Property Measurement of Nanofluid Droplets with Temperature Gradients," *Energies* 2020, 13, 244.

[11] Y.M. Nimdeo, A. Srivastava, “Understanding the temperature dependence of thermophysical properties of nanofluid suspensions using non-intrusive dynamic measurements,” *Exp. Therm. Fluid Sci.*, 94 (2018) 109–121.
[12] S.S. Rao, A. Srivastava, “Measuring thermal diffusivity of dilute nanofluids using interferometry-based inverse heat transfer approach,” *J. Thermophys. Heat Tran.*, 34 (3) (2020) 476–487.
[13] Touloukian, Y.S, Liley, P.E, & Saxena, S.C., *Thermophysical Properties of Matter- The TRPC Data Series. Volume 3. Thermal Conductivity – Nonmetallic Liquids and Gases*, 1970.
[14] G. Abbate, U. Bernini, E. Ragozzino, E. Somma, “The temperature dependence of the refractive index of water,” *Journal of Physics D: Applied Physics*, 11 (1978) 1167–1172.
[15] D. Naylor, “Recent developments in the measurement of convective heat transfer rates by laser interferometry,” *Int. J. Heat Fluid Flow*, 24 (3) (2003) 345–355.
[16] S. Sahamifar, D. Naylor, T. Yousefi, J. Friedman, “**Measurement of the thermal conductivity of nanofluids using a comparative interferometric method,”** *International Journal of Thermal Sciences*, 2024, 199, 108890.